Engineering the productivity of recombinant *Escherichia coli* for limonene formation from glycerol in minimal media

Christian Willrodt, Christian David, Sjef Cornelissen, Bruno Bühler, Mattijs K. Julsing and Andreas Schmid*

*Correspondence to:

Prof. Andreas Schmid

Laboratory of Chemical Biotechnology, Department of Biochemical and Chemical Engineering, TU Dortmund University, Emil-Figge-Straße 66, 44227 Dortmund, Germany

email: andreas.schmid@bci.tu-dortmund.de

Abbreviations

GPP: geranyl diphosphate, **FPP:** farnesyl diphosphate, **IPP:** isopentenyl diphosphate, **DMAPP:** dimethylallyl diphosphate, **LS:** *Mentha spicata* (*S*)-limonene synthase, **AGPPS2:** *Abies grandis* geranyl diphosphate synthase, **MVA:** mevalonate, **MEP:** 2-*C*-methyl-D-erythritol 4-phosphate/1-deoxy-D-xylulose 5-phosphate, **DINP:** diisononyl phtalate, **mg L_{org}^{-1}:** milligrams of limonene in the organic phase, **mg L_{aq}^{-1}:** milligrams of limonene in the aqueous phase , **STY:** space time yield, **1 U:** µmol of limonene formed per minute , **$Y_{p/x}$:** amount of limonene produced per amount of biomass formed, **$Y_{p/s}$:** amount of limonene produced per amount of substrate consumed

Keywords: white/industrial biotechnology, fermentation, monoterpene/limonene biosynthesis, *in vitro* and *in vivo* kinetics, reaction engineering

Submitted: 13-Jan-2014
Revised: 10-Mar-2014
Accepted: 21-Apr-2014

Abstract

The efficiency and productivity of cellular biocatalysts play a key role in the industrial synthesis of fine and bulk chemicals. This study focuses on optimizing the synthesis of (*S*)-limonene from glycerol and glucose as carbon sources using recombinant *E. coli*. The cyclic monoterpene limonene is extensively used in the fragrance, food, and cosmetic industries. Recently, limonene also gained interest as alternative jet fuel from biological origin.

Key parameters that limit the (*S*)-limonene yield related to genetics, physiology, and reaction engineering were identified. The growth-dependent production of (*S*)-limonene was shown for the first time in minimal media. *E. coli* BL21 (DE3) was chosen as the preferred host strain as it showed low acetate formation, fast growth, and high productivity. A two-liquid phase fed-batch fermentation with glucose as sole carbon and energy source resulted in the formation of 700 mg L_{org}^{-1} (*S*)-limonene. Specific activities of 75 mU g_{cdw}^{-1} were reached, but decreased relatively quickly. The use of glycerol as carbon source resulted in a prolonged growth and production phase (specific activities of ≥50 mU g_{cdw}^{-1}) leading to a final (*S*)-limonene concentration of 2,700 mg L_{org}^{-1}. Although geranyl diphosphate (GPP) synthase had a low solubility, its availability appeared not to limit (*S*)-limonene formation *in vivo* under the conditions investigated. GPP rerouting towards endogenous farnesyl diphosphate (FPP) formation did not limit (*S*)-limonene production either. The two-liquid phase fed-batch setup led to the highest monoterpene concentration obtained with a recombinant microbial biocatalyst to date.

Introduction

Recombinant whole-cell biocatalysts offer a broad range of possibilities for sustainable monoterpenoid synthesis based on the fermentation of renewable feedstocks. Monoterpenes are regarded as promising biosynthetic alternatives for jet fuel precursors [1-3] and building blocks for chemical [4, 5] and biocatalytic [6, 7] syntheses. The fermentative production of monoterpenes was previously demonstrated in recombinant *Escherichia coli* strains with an orthologous monoterpene biosynthesis pathway and grown either on defined rich [8] or complex medium [9-11]. The successful implementation of bacteria as organic synthesis catalysts requires detailed knowledge of the entire production system, including strain development, biocatalyst characterization, reaction and process engineering, as well as down-stream processing [12]. Moreover, the definition and analysis of strategies for improving efficiency and productivity provide a framework for further targeted bioprocess optimization to overcome biocatalyst and reaction related limitations [12, 13]. However, such a systematic approach has not yet been applied for the production of monoterpenes in *E. coli*.

Studies targeting the production of terpenes with recombinant microorganisms have mainly dealt with the engineering of strains that produced sesqui- [14-16], di- [17] and tetraterpenes [18, 19]. In contrast to sesquiterpenes and other larger terpenes, monoterpenes are almost exclusively found in plants rather than in microorganisms that are commonly used as biotechnological production strains [20]. This is due to the bacteria´s inability to produce the monoterpene precursor geranyl diphosphate (GPP). This obstacle has been overcome by the biotechnological introduction of GPP synthase and terpene cyclase genes into suitable *E. coli* strains [9]. However, physicochemical properties of monoterpenes, such as the high volatility, poor solubility in water [21], and toxicity [22] have remained a challenge on the reaction and process levels. The addition of an otherwise inert organic phase was shown to have a positive effect on *in situ* extraction of the products [23, 24]. Finally, the impact of the

microbial physiology on the performance of heterologous pathways involved in monoterpene formation - and vice versa – might be crucial [25]. A recent, an *in silico* profiling study using elementary mode analysis identified metabolic engineering strategies, beyond pathway engineering that have the potential to increase the monoterpenoid quantity in *E. coli* and *Saccharomyces cerevisiae* [26]. Unfortunately, this potential has not yet been exploited for the formation of monoterpenes.

The present study aims at defining and assessing of engineering strategies for the intensification of fermentative limonene production in *E. coli* (Fig. 1). A comprehensive multi-level analysis approach was used to investigate the properties of the biocatalyst as well as the reaction. The key parameters for engineering of the biotechnological monoterpene synthesis process were defined: (i) pathway construction, gene expression, and limited heterologous production of soluble and active proteins, (ii) kinetics of the enzymes involved, (iii) physiology (toxicity, competing reactions or pathways, intracellular fluxes), and (iv) technological aspects (limonene volatility, two-liquid-phase bioreactor setup, downstream processing). The systematic approach included metabolic engineering, host strain selection, along with reaction engineering, and resulted in the highest monoterpene titer produced with renewable feedstocks in in a recombinant bacterial strain to date.

Materials and Methods

Chemicals and bacterial strain

Anhydrous D-glucose was obtained from Alfa Aesar (Karlsruhe, Germany), and isopentenyl diphosphate (IPP) and dimethylallyl diphosphate (DMAPP) were purchased from Echelon Biosciences (Salt Lake City, UT, USA) with a purity >95%. Custom synthesized oligonucleotides were purchased from Sigma Aldrich (Steinheim, Germany). All other chemicals were obtained from AppliChem (Darmstadt, Germany), Sigma Aldrich (Steinheim, Germany), or Carl Roth (Karlsruhe, Germany) in the highest purity available. All *E. coli*

strains and plasmids used in this study are listed in Table 1. The antibiotics ampicillin, kanamycin, and/or chloramphenicol were applied at concentrations of 100 mg L^{-1}, 50 mg L^{-1} and 34 mg L^{-1}, respectively. Thiamine (if appropriate) was added to a final concentration of 0.001% (w/v).

Detailed information about vector construction and primer design (Table S1) are provided in the Supporting Information.

Cultivation of *E. coli* strains

5 mL of LB medium [27] were inoculated with *E. coli* from a frozen stock and incubated for 12 h at 37°C (200 rpm, 2.5 cm amplitude). Aliquots of 500 µL of the LB culture were transferred to 50 mL M9* medium with US* trace elements solution [28], 2 mM $MgSO_4$, and 0.5% (w/v) D-glucose and incubated for 16 - 20 h at 30°C in a baffled Erlenmeyer flask (200 rpm, 2.5 cm amplitude). This preculture was then used to inoculate fresh M9* medium supplemented with US* trace elements solution, 2 mM $MgSO_4$, and 0.5% (w/v) D-glucose at an optical density of 0.2 at 450 nm (OD_{450}). The culture was incubated at 30°C and gene expression was induced by adding 1.0 mM isopropyl β-D-1-thiogalactopyranoside (IPTG) or 0.2% L-arabinose, respectively once an OD_{450} of 0.6 (~0.1 g_{cdw} L^{-1}, cdw: cell dry weight) was reached. Incubation was continued at 20°C, 25°C, or 30°C.

Analytical Procedures

Cell growth was monitored by measuring turbidity (OD_{450}, Libra S11, Biochrom Ltd., Cambridge, UK, OD_{450} = 1 equals 0.166 g_{cdw} L^{-1}) [29].

Acetate formation and C source utilization were determined with HPLC analysis as described elsewhere [30]. In some instances, the glucose concentration was determined with a spectrophotometric assay kit (Enzytec, sciL Diagnostics, Viernheim, Germany).

Limonene concentrations were determined by GC using either a TRACE GC Ultra or Focus GC instrument (both from Thermo Fisher Scientific Inc., Waltham, MA, USA) equipped with

a flame ionization detector and a FactorFour-5ms column (30 m, 0.25 mm, 0.25 µm) (Varian, Inc., Palo Alto, CA, USA) and commercial (*S*)-limonene as standard (0.2 mM dodecane as internal standard). The settings were: injector temperature 250°C, splitless injection or split ratio 1:7, molecular nitrogen as carrier gas. Program: 80°C (5 min), 80 - 140°C (7.5°C min^{-1}), 140 - 300°C (40°C min^{-1}), 300°C (5 min).

Optical purity was determined by GC separation on a Finnigan Focus GC instrument equipped with a chiral Supelco β-DEX 120 column (Sigma Aldrich, Steinheim, Germany). Program: 50°C (5 min), 80 - 140°C (5°C min^{-1}), 140 - 230°C (40°C min^{-1}), 230°C (5 min).

Limonene and by-products were determined with GC-MS using a CP3800 GC coupled to a 1200 Quadrupole MS (Varian, Inc., Palo Alto, CA, USA) using the same column and settings as above.

^{1}H-NMR spectra were recorded in chloroform-d1 using a Bruker DRX-400 spectrometer (Bruker, Billerica, MA, USA) with a 5 mm sample head (400.13 MHz).

***In vitro* limonene formation assay**

Fully induced *E. coli* cells were harvested by centrifugation (20 min, 4°C, 4,618 *g*), resuspended in 5 mL buffer A (0.05 mM potassium phosphate buffer, pH 7.4, 5% (v/v) glycerol, 1 mM dithiothreitol, 15 mM $MgCl_2$) and disrupted by three passages through a French press (5.5 MPa, SLM-Aminco, Rochester, NY, USA). The solution was subsequently diluted to 0.5 $g_{protein}$ L^{-1} (Bradford assay [31]) in buffer A, aliquoted and incubated (5 min, 30°C, 1000 rpm, Thermomixer Comfort, Eppendorf, Hamburg, Germany). Bioconversion was started by adding 60 µL of an equimolar mixture of IPP and DMAPP (0.5 g L^{-1} each in ethanol). The reaction was terminated by adding a saturating amount of NaCl and ice-cold Et_2O (containing 0.2 mM dodecane as internal standard), and mixing vigorously for 30 s. The organic and aqueous phases were separated by centrifugation (5 min, 4°C, 17,000 *g*) and the

organic phase was subsequently dried over anhydrous Na_2SO_4 prior to determining the limonene concentration by GC analysis.

***In vivo* limonene formation assay**

E. coli strains were grown at 30°C as described above, but in screw-capped baffled flasks (250 mL). Together with 1 mM IPTG, 10 mL diisonoylphtalate (DINP) were added as inert organic carrier phase to 40 mL of the culture. For sampling, the phases were separated by centrifugation (5 min, 4°C, 17,000 *g*). Prior to GC analysis, the organic phase was diluted in Et_2O with 0.2 mM dodecane and dried over anhydrous Na_2SO_4.

Fermentative production of limonene in a stirred-tank reactor

Two-liquid phase fermentations were carried out in 3.1 L stirred tank reactors (KLF 2000, Bioengineering, Wald, Switzerland) equipped with two Rushton turbine stirrers. For batch cultivation, 1.0 L M9 medium, supplemented with chloramphenicol, ampicillin, US* trace elements [28], $MgSO_4$, and 1.5 % (w/v) carbon source (D-glucose or glycerol) was inoculated to an OD_{450} of 0.2 with an overnight M9* preculture of *E. coli* BL21 (DE3) (pMVAidi, pTAC:LS:AGPPS2). The pH was set to 7.2 and automatically controlled by titration with either 15% (v/v) phosphoric acid or 25% (v/v) ammonium hydroxide solution. Batch cultures were incubated for 16 h or 20 h until depletion of the carbon source (30°C, aeration rate 1 vvm, 1800 rpm).

After the addition of 1 mL 1000x US* trace element stock solution, a carbon-limited and controlled exponential feed with either 73% (w/v) glucose or glycerol as carbon source (both containing 19.6 g L^{-1} $MgSO_4$) was started to keep the exponential growth rates between 0.15 h^{-1} and 0.18 h^{-1}. After reaching a biomass concentration of 20 g_{cdw} L^{-1} the feed rate was kept constant. The pO_2-value was kept >30% saturation by adjusting the stirrer speed. After two hours of exponential feed, 0.5 L of DINP were added and gene expression was induced by adding 1 mM IPTG. Immediate changes in the O_2 saturation upon interruptions of the feed

at regular intervals were taken as an indication that the carbon source was not accumulating in the medium. GC analysis samples were prepared as described above.

Purification of (*S*)-limonene

For isolation of limonene, the fermentation broth was centrifuged (15 min, 4°C, 4,700 *g*) and the aqueous phase was removed. The resulting emulsion was immediately frozen (-80°C, 1 h) and centrifuged again (20 min, 4°C, 4,700 g) after thawing. 120 mL of the clear organic phase were distilled under reduced pressure (4 - 6 mbar, ~160°C).

Results

Limonene synthesis in recombinant *E. coli.* The synthesis of limonene in recombinant *E. coli* requires the functional expression of two plant genes. The expression vectors pBAD:LS and pET24:AGPPS2 were equipped with (see Supporting Information for details) the truncated and codon-optimized genes for limonene synthase (LS) from *Mentha spicata* and GPP synthase 2 (AGPPS2) from *Abies grandis*, respectively. These two expression systems were chosen, as their use previously led to functional expression of GPP synthase and limonene synthase without codon-optimization in *E. coli* [9]. In addition, a putative bacterial GPP synthase (pET24:KO) from *Streptomyces* sp. strain KO-3988 [32] was investigated.

Membrane-free extracts were prepared from induced *E. coli* BL21 (DE3) cells that contained either pBAD:LS/pET24:AGPPS2 or pBAD:LS/pET24:KO. With GPP as substrate, activities of 1.6 and 3.6 U $g_{protein}^{-1}$ were observed. When using IPP and DMAPP, activities for the two-step bioconversion were 0.13 and 0.15 U $g_{protein}^{-1}$. Thus, the introduced genes were functionally expressed and there was no significant difference in performance between the GPP synthase enzymes from *A. grandis* and *Streptomyces* sp. strain KO3988 .

E. coli BL21 (DE3) (pBAD:LS, pET24:AGPPS2) and *E. coli* BL21 (DE3) (pBAD:LS, pET24:KO) were tested subsequently for their ability to produce limonene with glucose as C source. No limonene was detected (detection limit ~0.3 mg L^{-1}) in the culture supernatant of

either strain after cultivation for 24 h in M9* medium, which was in contrast to an earlier study reporting the formation of ~6 mg L^{-1} limonene [9]. Limonene evaporation may explain the negative result. Therefore, the non-toxic organic solvent DINP [23] was added to the cultures during growth for the purpose of *in situ* extraction. The organic phase subsequently accumulated limonene (~0.4 mg L_{aq}^{-1} in 72 h for both strains), demonstrating that limonene was produced from glucose, albeit at low quantity.

Host effects of different *E. coli* metabolic backgrounds. The first strategy to optimize the biocatalyst was to increase precursor supply, an optimization strategy that has shown to be successful for the production of the sesquiterpene amorpha-4,11-diene in *E. coli* [16] and was very recently also applied to the production of limonene [8]. In order to increase the intracellular availability of IPP and DMAPP, the orthologous mevalonate (MVA) pathway from *S. cerevisiae* was also introduced [16]. All the genes of the MVA pathway, that convert endogenous acetyl-CoA into IPP and DMAPP (Fig. 1) were assembled on the plasmid pMVAidi. A second plasmid, pTAC:LS:AGPPS2, contained the genes for LS and AGPPS2. Three K-12-derived *E. coli* strains (DH5α, JM101, and MG1655) and the B strain *E. coli* BL21 (DE3) were transformed with pMVAidi and pTAC:LS:AGPPS2 and cultivated in the presence of DINP. Limonene was produced in all strains with final yields ranging from 15 to 25 mg L_{aq}^{-1} after 78 h (Fig. 2). Introducing the MVA pathway and simultaneously putting the downstream genes under the control of a tac-promoter on one plasmid, resulted in over 60-fold higher limonene concentrations as compared to the *E. coli* strain BL21 (DE3) harboring the incompatible plasmids pBAD:LS and pET24:AGPPS2 that was initially used. These results clearly confirmed that endogenous precursor supply was a limiting factor for monoterpenoid synthesis in the four *E. coli* strains investigated.

The specific limonene yield relative to the biomass after 50 h of cultivation was highest for *E. coli* DH5α (12.0 ± 2.2 mg g_{cdw}^{-1}) and for *E. coli* MG1655 (12.2 ± 0.5 mg g_{cdw}^{-1})

(Table 2). The yields relative to the carbon source for *E. coli* DH5α and *E. coli* MG1655 were 1.9 ± 0.4 mg g^{-1} and 2.0 ± 0.1 mg g^{-1}, respectively, which translate into approximately 0.6% of the theoretically achievable maximum (calculated to be ~0.32 $g_{limonene}$ $g_{glucose}^{-1}$ [2]) (Table 2).

Different limonene formation kinetics were observed in the E. *coli* strains, and acetate concentrations appeared to correlate with the level of limonene formation. *E. coli* DH5α produced the highest amount of acetate (5.25 g L^{-1}) and simultaneously also showed the highest limonene concentration after 30 h (19.53 ± 0.75 mg L_{aq}^{-1}) (Fig. 2A). In contrast, *E. coli* JM101 showed low amounts of acetate (3.22 g L^{-1}) and also yielded the lowest limonene concentration after 30 h (10.88 ± 0.43 mg L_{aq}^{-1}) (Fig. 2C). The biomass concentrations of 1.69 g_{cdw} L^{-1} for *E. coli* JM101 and 1.54 g_{cdw} L^{-1} for *E. coli* DH5α were similar for both strains, but the glucose uptake rate during logarithmic growth was highest for *E. coli* JM101 (~2.4 mmol g_{cdw}^{-1} h^{-1}). In order to test whether acetate formation had an influence on limonene formation, an *E. coli* strain that lacked the phosphotransacetylase (*pta*) gene that converts acetyl-CoA into acetylphosphate was investigated. *E. coli* MG1655 DE3 (Δ*pta*, Δ*ldhA*, Δ*adhE*) (pMVAidi, pTAC:LS:AGPPS2) produced less limonene (9.07 ± 0.34 g L_{aq}^{-1}) and less acetate (0.85 g L^{-1}) than the strains with a functional *pta* gene under the same experimental conditions (Fig. 3). The lack of a functional *pta* gene and the resulting physiological properties of the cell prevented an increased flux of metabolites towards limonene production. Thus, *E. coli* BL21 (DE3) was selected as the preferred host strain for subsequent experiments as it showed fast growth, a high limonene productivity (15.2 ± 2.4 mg L^{-1} in 30 h) and low formation of acetate, which is generally considered detrimental for growth and gene expression.

Native FPP synthase activity does not compete with GPP synthase for endogenous IPP and DMAPP. *E. coli* produces the sesquiterpene precursor farnesyl diphosphate (FPP) via an

endogenous FPP synthase. FPP is required for the synthesis of essential compounds such as menaquinone and ubiquinone, which can be of benefit for terpenoid biosynthesis. However, as far as the production of monoterpenes is concerned, the introduction of a recombinant GPP synthase enzyme might have an impact on the cellular metabolism of the host, and render monoterpene production difficult due to ongoing endogenous sesquiterpene synthesis. The intracellular GPP concentration might be limited due to rerouting of IPP and DMAPP or GPP towards the formation of FPP by native FPP synthase (*ispA*). A literature search revealed that the *Michaelis* constant (K_M) of the *E. coli* FPP synthase is 10-fold lower for IPP (2-fold for DMAPP) than the K_M of the *A. grandis* GPP synthase (Table 3) [33, 34]. To investigate the possible competition between FPP synthase and GPP synthase, limonene formation was analyzed in an *ispA* (encoding FPP synthase) deficient *E. coli* W3110 SF7N and its isogenic control *E. coli* W3110 SF5 [35], both harboring pTAC:AGPPS2 and pMVAidi. After depletion of glucose, both strains reached similar biomass concentrations of $1.19 \pm 0.07\ g_{cdw}\ L^{-1}$ (SF7N) and $1.17 \pm 0.09\ g_{cdw}\ L^{-1}$ (SF5) and similar product levels (19.05 ± 0.37 mg L_{aq}^{-1} for *E. coli* SF7N and 20.6 ± 0.7 mg L_{aq}^{-1} for *E. coli* SF5) (Fig. 4). Different acetate levels were not expected, given the near 100% genetic identity of the two strains. Hence, despite favored kinetic parameter, endogenous FPP synthesis did not affect monoterpene yield by limiting the terpenoid precursors IPP, DMAPP, and GPP.

Does GPP synthase activity limit limonene formation rate? SDS-PAGE analyses with protein extracts from fully induced strains showed that *E. coli* JM101 produced more GPP synthase than *E. coli* BL21 (DE3) (Fig S1). Additionally, lower (soluble) GPP synthase levels were observed in *E. coli* BL21 (DE3) at 30°C and 25°C compared to 20°C, demonstrating that the translation, protein folding and/or protein stability was temperature-dependent (Fig. S1). Extracts derived from *E. coli* BL21 (DE3) (pTAC:LS:AGPPS2) (Fig. 5A) and *E. coli* BL21 (DE3) (pMVAidi, pTAC:LS:AGPPS2) cultivated at 25°C showed specific activities of

1.0 ± 0.0 U $g_{protein}^{-1}$ and 1.2 ± 0.0 U $g_{protein}^{-1}$ respectively for the two-step bioconversion of IPP and DMAPP to limonene. After cultivation at 20°C, the extracts showed higher specific limonene formation rates of 2.1 ± 0.0 U $g_{protein}^{-1}$ (pTAC:LS:AGPPS2) (Fig. 5A) and 4.0 ± 0.1 U $g_{protein}^{-1}$ (pMVAidi, pTAC:LS:AGPPS2). Raising the expression temperature to 30°C led to a further reduction in limonene formation rates (data not shown), most likely caused by the decreasing level of soluble AGPPS2 (Fig. S1) as the temperature increased. In contrast, no significant temperature-dependent difference in limonene formation was observed with extracts derived from fully induced *E. coli* JM101 (pTAC:LS:AGPPS2) cells (Fig. 5C). The presence of the additional pMVAidi plasmid did not obviously impair the expression of AGPPS2 and LS genes. In order to adress the impact of different amounts of AGPPS2 on whole-cell limonene formation, the strains (with both plasmids) were cultivated at different temperatures. When using glucose as carbon source, the specific *in vivo* limonene yield increased with increasing temperature for *E. coli* BL21 (DE3), whereas it remained constant in *E. coli* JM101 (Fig. 5B and 5D). The limonene yield of *E. coli* BL21 (DE3) at 20°C was only 33.1 ± 10.7% of the amount observed at 30°C. In contrast, *E. coli* JM101 produced at 20°C 92.3 ± 7.7% of the quantity formed at 30°C. The biomass yields were similar in all cases, with averaged final concentrations of 1.19 g_{cdw} L^{-1} (± 6%) for *E. coli* BL21 (DE3) and 1.39 g_{cdw} L^{-1} (± 14%) for *E. coli* JM101. Glucose was metabolized entirely in all fermentations (Table S2). Since the quantity of soluble AGPPS2 in *E. coli* BL21 (DE3) was reduced at elevated temperatures (Fig. S1), it did not correlate with the *in vivo* limonene formation yield. As the largest part of limonene was produced within 24 h after induction (Fig. 2A), we therefore conclude, that AGPPS2 activity did not limit overall limonene production under the selected experimental conditions. For *E. coli* BL21 (DE3), the ratio of the limonene yields achieved in strains with and without the MVA pathway ($Y_{p/x\ (MVA)}$ / $Y_{p/x\ (non\ MVA)}$) increased with rising temperatures from 11 (20°C) to 19 (30°C).

The reduced *in vivo* limonene formation in *E. coli* BL21 (DE3) at 20°C and 25°C can therefore be explained by the reduced performance of one or more MVA pathway enzymes. However, the differences observed in AGPPS2 solubility at different temperatures and in different hosts, might allow for further optimization of a the production process.

Gram scale production and purification of (*S*)-limonene

With the aim of achieving gram-scale amounts of (*S*)-limonene from cheap and renewable carbon sources *E. coli* BL21 (DE3) (pMVAidi, pTAC:LS:AGPPS2) was cultivated in a technical scale process (3.1 L) using a two-liquid phase fed-batch approach with either glucose or glycerol as carbon source and DINP as organic carrier solvent (phase ratio 1:2). With glycerol as sole carbon source, a final limonene concentration of 2.7 g L_{org}^{-1} (grams limonene per liter organic phase) was achieved within 45 h (Fig. 6A), which was 3.9-fold higher than the final limonene concentration achieved with glucose as carbon source (0.69 g L_{org}^{-1}) (Fig. 6B). Furthermore, a 26% higher final biomass concentration of 61.8 g_{cdw} L^{-1} was achieved with glycerol than with glucose (49.1 g_{cdw} L^{-1}). The increased limonene concentration is not therefore just attributable to the increase in biomass formation. Since the protein levels of LS and AGPPS2 were similar in the glucose- and glycerol-based experiments (as indicated by PAGE analysis, data not shown), it was concluded that the higher limonene concentration under glycerol-limited growth was not caused by the higher activity of the heterologously expressed limonene synthesis pathway but by other metabolic factors, such as ATP and redox equivalent regeneration rates.

The initial specific limonene formation rates were low in both fed-batch cultivation experiments but increased to approximately 70 mU g_{cdw}^{-1} (with glucose) during the first eight hours (Fig. 6C). During fed-batch cultivation with glucose as carbon source, the specific limonene formation rate remained constant during the subsequent 7 hours before decreasing to 7 mU g_{cdw}^{-1} after 32 h. This decrease in the limonene formation rate is most likely due an as

yet unidentified metabolic inactivation of the cells (glucose accumulation). With glycerol as carbon source, the high limonene formation rate remained almost constand during the entire fermentation process (~45 h), reaching specific activities of more than 50 mU g_{cdw}^{-1} (Fig. 6C). These fed-batch experiments demonstrate that the selection of the appropriate substrate and reaction setup is crucial for optimizing product yields. Limonene obtained in the fed-batch experiment with glucose as carbon source was purified via distillation. The resulting distillate (42% isolation yield) had a characteristic odor, contained (*S*)-limonene with an enantiomeric excess (*ee*) of ≥ 99.8, and exhibited a purity of ≥ 96% as determined by GC and ^{1}H-NMR, respectively. Impurity traces of the monoterpenes β-pinene and myrcene were also identified.

Discussion

Whole-cell biocatalyst engineering for monoterpene production

Over the past decade, extensive research efforts have been undertaken to construct recombinant microbial platform organisms that enable the fermentative production of terpenoids. Recent achievements in synthetic biology and metabolic engineering constitute a first step towards the rational design of microbial cell factories that are able to produce the desired terpenoids from cheap and renewable resources [36]. However, knowledge about the regulatory mechanisms involved at the genetic and protein levels, and potential limitations resulting from inhibitions, the toxicity of components or interference of substrates and products with transcription factors is still very limited. This is particularly true when genes or entire pathways of foreign organisms are utilized [25]. Furthermore, with respect to monoterpenoid formation, previous studies have rarely addressed parameters such as productivity (mg L^{-1} h^{-1}), specific activity (U $gcdw^{-1}$) or specific yield (mg $gcdw^{-1}$), which are, however, also highly important.

The presence of a competing pathway (FPP synthase) and a mainly insoluble GPPS at 30°C did not affect the amount of limonene produced *in vivo*. The main limitation of (mono)terpene production in recombinant *E. coli* appeared to be the availability of the terpene precursors IPP and DMAPP. The limonene concentrations obtained in shake flasks with glucose as carbon source (15-25 mg L_{aq}^{-1} of limonene) were of the same order of magnitude as those previously reported for the heterologous production of limonene in *E. coli* DH1 [8] that was engineered in a similar way to the strains used in this study and that was grown in a defined rich medium. A significant optimization potential was documented when all required heterologous pathway genes were combined on one plasmid, and when the heterologous MVA pathway was further optimized with respect to codon usage, promotor strength and selection of an appropriate source organism for the required genes [8].

E. coli strains derived from K-12, harboring an optimized 2-C-methyl-D-erythritol 4-phosphate (MEP) pathway, showed a 2.5-fold increased taxadiene (diterpene) production compared to the respective B strain variants [37]. In the present study, the selection of strains that were able to synthesize monoterpenoids via the heterologous MVA pathway does not appear to be the crucial factor, as all strains investigated produced similar amounts of limonene (± 25%). (Fig. 2, Table 2). One explanation might be that in contrast to the eukaryotic MVA pathway, the MEP pathway originates from *E. coli* and is thus better suited to meet the intrinsic regulatory requirements of the host. High levels of acetate and the highest limonene concentration were found for *E. coli* DH5α harboring the limonene formation pathway (Fig. 2). This was unexpected, as acetate formation is a sink for acetyl-CoA and was therefore assumed to be a competing pathway for the production of terpenoids. Nevertheless, a reasonable explanation for the correlation between acetate (leading to the generation of 1 mole ATP per mole acetate) and limonene formation may be seen in the activity of the exogenously introduced MVA pathway. This pathway requires 6 moles of ATP for the

formation of 1 mole limonene, which might cause a significant metabolic burden. Although the final limonene concentration might seem low, the accumulation of (toxic) intermediates resulting from imbalances in the pathway, as well as the energy (and redox equivalents) required for expression of the genes involved, may increase the ATP demand even further. We therefore conclude that shortage of acetyl-CoA is does not limit the limonene production rate in *E. coli* under these specific experimental conditions. A similar finding was recently published for the biosynthetic production of long-chain fatty acids in *E. coli* that also starts from acetyl-CoA [38]. The knocking out of the two key genes of the acetate formation pathway, *ack-pta* (acetate kinase/phosphotransacetylase) and *poxB* (pyruvate oxidase) did not result in increased fatty acid concentrations [38].

Reaction engineering: two-liquid phase setup

Several studies have described a two-liquid phase approach for the *in situ* extraction of the terpenoids produced [39, 40]. Although an earlier study reported the production of limonene in *E. coli* in an aqueous medium alone [9], the addition of a second organic phase appeared to be a mandatory requirement in our experiments that were aimed at avoiding evaporation and facilitating limonene quantification. Loss of product by evaporation was proven by the fact that exogenously added limonene (100 μM) could no longer be detected by means of GC analysis (detection limit ~0.3 mg L^{-1}) after incubation for 4 h at 30°C and orbital shaking in M9* medium. DINP was found to be best suited for the two-liquid-phase setup, since it is reported to have no significant impact on the growth rate of *E. coli* [23] and shows a favorable limonene partition coefficient ($24.0 \pm 2.7 \times 10^3$). In fact, the addition of DINP was beneficial in our experiments with respect to the prevention of limonene evaporation. The efficient extraction of the product also facilitated downstream product purification by distillation and most likely also decreased the toxic effects of limonene on the host cell.

Reaction engineering: glycerol as sole carbon source

Glycerol as carbon source in fed-batch cultivation yielded a four-fold higher limonene concentration compared to glucose (Fig. 6). The beneficial effect of glycerol as sole or supplementary carbon source has been reported before for the fermentative production of carotenoids in MEP-engineered *E. coli* strains [41-43] and for sesquiterpenes in a MVA-engineered *E. coli* strain [16]. However, the reasons for the reduced concentrations in the presence of glucose, remained unclear [41]. In the present study, the stability of the whole-cell biocatalyst was shown to be responsible for the elevated limonene concentration observed in the glycerol-based fermentation (Fig. 7). The stabilizing effect of glycerol on isolated enzymes is well known [44, 45]. For whole-cell biocatalysis, however, metabolic effects rather than direct enzyme stabilization are to be expected. In general terms, glycerol exhibits a higher degree of reduction ($\kappa = 0.47$) per carbon atom as compared to glucose ($\kappa = 0.40$) [46]. It may therefore be beneficial for the formation of highly reduced compounds such as limonene ($\kappa = 0.56$). Furthermore, the incorporation of glycerol into biomass might result in the formation of additional reducing equivalents [46].

Production rates and product yields

The total productivities (or space time yields, STY) over the entire fed-batch cultivation periods were calculated as 5.6 mg L_{aq}^{-1} h^{-1} and 22.6 mg L_{aq}^{-1} h^{-1} for cells grown with glucose or glycerol as carbon source, respectively. The productivity observed for the glycerol-based experiment equals roughly one fourth of the productivity that is considered a threshold for developing a profitable production process for fine chemicals (100 mg L^{-1} h^{-1}) [47]. Considering the maximum space time yields observed (~40 mg L_{aq}^{-1} h^{-1} for the glycerol-limited cultivation), the rates are only 2.5-fold lower than the required minimum proposed for industrial application.

The specific limonene formation rates for *E. coli* BL21 (DE3) in fed-batch (75 mU g_{cdw}^{-1}) and batch cultivation during exponential growth phase (85 mU g_{cdw}^{-1}) were similar. Despite these promising results, the limonene yields based on the carbon source utilized during fed-batch cultivation were still rather low and were calculated to be 1.31 mg g^{-1} and 4.10 mg g^{-1} when using glucose or glycerol as carbon source, respectively. These values translate into 0.45% and 1.0% of the theoretically achievable maximum (stoichiometric calculation), and are thus also similar to the yields obtained for *E. coli* BL21 (DE3) in batch cultivation (Table 2). Nevertheless, it has to be taken into account that a large proportion of the carbon utilized is directed towards the production of biomass and by-products. It might therefore be useful for future applications to decouple product and biomass formation.

Conclusions

The optimization of whole-cell processes requires a systematic analysis of the biocatalyst, e.g. the microbial cell, in the reaction process. In order to optimize the fermentative production of (*S*)-limonene in recombinant *E. coli*, the key engineering parameters were defined and analyzed at the genetic (pathway engineering, gene expression), physiological (toxicity, competing pathways), and technological (volatility, two-liquid phase reactor setup, downstream processing) levels. This systematic approach allowed the identification of the parameters that play a key role in monoterpene production, and subsequently the development of strategies for bioprocess optimization. In accordance with earlier studies, orthologous pathway engineering was crucial to overcoming limiting quantities of terpene precursors. This potential was successfully exploited in earlier studies [8, 11]. Maximizing productivity and stability of the microbial biocatalyst is also highly important. This can be achieved by specifically engineering the host strain and by modifying the reaction conditions. The results of the present study furthermore showed that mass transfer rates of oxygen and glycerol into the cells were not restrictive. This provides a basis to further optimize productivity by

exploiting the potential of the whole-cell biocatalyst. Future process improvement should also focus on the optimization of intracellular metabolite fluxes towards acetyl-coA, the supply of sufficient redox and energy equivalents, as well as cultivation and production conditions.

Acknowledgements

We would like to thank Stefan Konieczny (BMP, TU Dortmund University) for assistance with the vacuum distillation of limonene and NMR analysis. Kristala L. Jones-Prather (MIT, Cambridge, MA, USA) and Shingo Fujisaki (Toho University, Funabashi, Chiba, Japan) generously provided *E. coli* MG1655 (DE3) (Δ*pta*, Δ*ldhA*, Δ*adhE*) and *E. coli* W3110 SF7N and SF5, respectively. The project was funded by the Deutsche Bundestiftung Umwelt (DBU: AZ13252 and AZ20006/855).

The authors declare no commercial or financial conflict of interest.

References

[1] Harvey, B. G., Wright, M. E., Quintana, R. L., High-density renewable fuels based on the selective dimerization of pinenes. *Energ. Fuel.* 2009, *24*, 267-273.
[2] Dunlop, M. J., Dossani, Z. Y., Szmidt, H. L., Chu, H. C.*, et al.*, Engineering microbial biofuel tolerance and export using efflux pumps. *Mol. Syst. Biol.* 2011, *7*, 10.1038/msb.2011.1021.
[3] Bokinsky, G., Peralta-Yahya, P. P., George, A., Holmes, B. M.*, et al.*, Synthesis of three advanced biofuels from ionic liquid-pretreated switchgrass using engineered *Escherichia coli*. *Proc. Natl. Acad. Sci. USA* 2011, *108*, 19949-19954.
[4] Wender, P. A., Bi, F. C., Brodney, M. A., Gosselin, F., Asymmetric synthesis of the tricyclic core of NGF-inducing cyathane diterpenes via a transition-metal-catalyzed [5+2] cycloaddition. *Org. Lett.* 2001, *3*, 2105-2108.
[5] Thomas, A. F., Bessiere, Y., Limonene. *Nat. Prod. Rep.* 1989, *6*, 291-309.
[6] Mirata, M. A., Heerd, D., Schrader, J., Integrated bioprocess for the oxidation of limonene to perillic acid with *Pseudomonas putida* DSM 12264. *Process Biochem.* 2009, *44*, 764-771.
[7] van Beilen, J. B., Holtackers, R., Luscher, D., Bauer, U.*, et al.*, Biocatalytic production of perillyl alcohol from limonene by using a novel *Mycobacterium* sp. cytochrome P450 alkane hydroxylase expressed in *Pseudomonas putida*. *Appl. Environ. Microbiol.* 2005, *71*, 1737-1744.
[8] Alonso-Gutierrez, J., Chan, R., Batth, T. S., Adams, P. D.*, et al.*, Metabolic engineering of *Escherichia coli* for limonene and perillyl alcohol production. *Metab. Eng.* 2013, *19*, 33-41.
[9] Carter, O. A., Peters, R. J., Croteau, R., Monoterpene biosynthesis pathway construction in *Escherichia coli*. *Phytochemistry* 2003, *64*, 425-433.
[10] Reiling, K. K., Yoshikuni, Y., Martin, V. J., Newman, J.*, et al.*, Mono and diterpene production in *Escherichia coli*. *Biotechnol. Bioeng.* 2004, *87*, 200-212.
[11] Yang, J., Nie, Q., Ren, M., Feng, H.*, et al.*, Metabolic engineering of *Escherichia coli* for the biosynthesis of alpha-pinene. *Biotechnol. Biofuels* 2013, *6*, 60-69.
[12] Kuhn, D., Blank, L. M., Schmid, A., Buehler, B., Systems biotechnology – Rational whole-cell biocatalyst and bioprocess design. *Eng. Life Sci.* 2010, *10*, 384-397.
[13] Meyer, D., Buehler, B., Schmid, A., Process and catalyst design objectives for specific redox biocatalysis, in: Sariaslani, S., Gadd, G. M., Laskin, A. (Eds.), *Advances in Applied Microbiology*, Elsevier 2006, pp. 53-91.
[14] Tsuruta, H., Paddon, C. J., Eng, D., Lenihan, J. R.*, et al.*, High-level production of amorpha-4,11-diene, a precursor of the antimalarial agent artemisinin, in *Escherichia coli*. *PLoS One* 2009, *4*, 10.1371/journal.pone.0004489.
[15] Pitera, D. J., Paddon, C. J., Newman, J. D., Keasling, J. D., Balancing a heterologous mevalonate pathway for improved isoprenoid production in *Escherichia coli*. *Metab. Eng.* 2007, *9*, 193-207.
[16] Martin, V. J., Pitera, D. J., Withers, S. T., Newman, J. D., Keasling, J. D., Engineering a mevalonate pathway in Escherichia coli for production of terpenoids. *Nature biotechnology* 2003, *21*, 796-802.
[17] Ajikumar, P. K., Xiao, W. H., Tyo, K. E., Wang, Y.*, et al.*, Isoprenoid pathway optimization for Taxol precursor overproduction in *Escherichia coli*. *Science* 2010, *330*, 70-74.
[18] Yoon, S. H., Lee, S. H., Das, A., Ryu, H. K.*, et al.*, Combinatorial expression of bacterial whole mevalonate pathway for the production of beta-carotene in *E. coli*. *J. Biotechnol.* 2009, *140*, 218-226.
[19] Alper, H., Stephanopoulos, G., Uncovering the gene knockout landscape for improved lycopene production in *E. coli*. *Appl. Microbiol. Biotechnol.* 2008, *78*, 801-810.

[20] Fischer, M. J., Meyer, S., Claudel, P., Bergdoll, M., Karst, F., Metabolic engineering of monoterpene synthesis in yeast. *Biotechnol. Bioeng.* 2011, *108*, 1883-1892.
[21] Schmid, C., Steinbrecher, R., Ziegler, H., Partition coefficients of plant cuticles for monoterpenes. *Trees - Struct. Funct.* 1992, *6*, 32-36.
[22] Brennan, T. C., Turner, C. D., Kromer, J. O., Nielsen, L. K., Alleviating monoterpene toxicity using a two-phase extractive fermentation for the bioproduction of jet fuel mixtures in *Saccharomyces cerevisiae*. *Biotechnol. Bioeng.* 2012, *109*, 2513-2522.
[23] Schewe, H., Holtmann, D., Schrader, J., P450(BM-3)-catalyzed whole-cell biotransformation of alpha-pinene with recombinant *Escherichia coli* in an aqueous-organic two-phase system. *Appl. Microbiol. Biotechnol.* 2009, *83*, 849-857.
[24] Cornelissen, S., Julsing, M. K., Volmer, J., Riechert, O.*, et al.*, Whole-cell-based CYP153A6-catalyzed (S)-limonene hydroxylation efficiency depends on host background and profits from monoterpene uptake via AlkL. *Biotechnol. Bioeng.* 2013, *110*, 1282-1292.
[25] Kim, J., Copley, S. D., Inhibitory cross-talk upon introduction of a new metabolic pathway into an existing metabolic network. *Proc. Natl. Acad. Sci. USA* 2012, *109*, 2856-2864.
[26] Gruchattka, E., Hadicke, O., Klamt, S., Schutz, V., Kayser, O., In silico profiling of *Escherichia coli* and *Saccharomyces cerevisiae* as terpenoid factories. *Microb. Cell. Fact.* 2013, *12*, 10.1186/1475-2859-1112-1184.
[27] Sambrook, J., Russel, D. W., *Molecular cloning. A laboratory manual*, Cold Spring Harbor Laboratory Press, New York 2001.
[28] Panke, S., Meyer, A., Huber, C. M., Witholt, B., Wubbolts, M. G., An alkane-responsive expression system for the production of fine chemicals. *Appl. Environ. Microbiol.* 1999, *65*, 2324-2332.
[29] Blank, L. M., Ebert, B. E., Buehler, B., Schmid, A., Metabolic capacity estimation of *Escherichia coli* as a platform for redox biocatalysis: constraint-based modeling and experimental verification. *Biotechnol. Bioeng.* 2008, *100*, 1050-1065.
[30] Gross, R., Lang, K., Buehler, K., Schmid, A., Characterization of a biofilm membrane reactor and its prospects for fine chemical synthesis. *Biotechnol. Bioeng.* 2010, *105*, 705-717.
[31] Zor, T., Selinger, Z., Linearization of the Bradford protein assay increases its sensitivity: theoretical and experimental studies. *Anal. Biochem.* 1996, *236*, 302-308.
[32] Kawasaki, T., Hayashi, Y., Kuzuyama, T., Furihata, K.*, et al.*, Biosynthesis of a natural polyketide-isoprenoid hybrid compound, furaquinocin A: identification and heterologous expression of the gene cluster. *J. Bacteriol.* 2006, *188*, 1236-1244.
[33] Fujisaki, S., Nishino, T., Katsuki, H., Isoprenoid synthesis in *Escherichia coli*. Separation and partial purification of four enzymes involved in the synthesis. *J. Biochem.* 1986, *99*, 1327-1337.
[34] Burke, C., Croteau, R., Geranyl diphosphate synthase from *Abies grandis*: cDNA isolation, functional expression, and characterization. *Arch. Biochem. Biophys.* 2002, *405*, 130-136.
[35] Fujisaki, S., Takahashi, I., Hara, H., Horiuchi, K.*, et al.*, Disruption of the structural gene for farnesyl diphosphate synthase in *Escherichia coli*. *J. Biochem.* 2005, *137*, 395-400.
[36] Keasling, J. D., Synthetic biology and the development of tools for metabolic engineering. *Metab. Eng.* 2012, *14*, 189-195.
[37] Boghigian, B. A., Salas, D., Ajikumar, P. K., Stephanopoulos, G., Pfeifer, B. A., Analysis of heterologous taxadiene production in K- and B-derived *Escherichia coli*. *Appl. Microbiol. Biotechnol.* 2012, *93*, 1651-1661.
[38] Li, M., Zhang, X., Agrawal, A., San, K. Y., Effect of acetate formation pathway and long chain fatty acid CoA-ligase on the free fatty acid production in *E. coli* expressing acy-ACP thioesterase from *Ricinus communis*. *Metab. Eng.* 2012, *14*, 380-387.

[39] Newman, J. D., Marshall, J., Chang, M., Nowroozi, F.*, et al.*, High-level production of amorpha-4,11-diene in a two-phase partitioning bioreactor of metabolically engineered *Escherichia coli*. *Biotechnol. Bioeng.* 2006, *95*, 684-691.
[40] Morrone, D., Lowry, L., Determan, M. K., Hershey, D. M.*, et al.*, Increasing diterpene yield with a modular metabolic engineering system in *E. coli*: comparison of MEV and MEP isoprenoid precursor pathway engineering. *Appl. Microbiol. Biotechnol.* 2010, *85*, 1893-1906.
[41] Lee, P. C., Mijts, B. N., Schmidt-Dannert, C., Investigation of factors influencing production of the monocyclic carotenoid torulene in metabolically engineered *Escherichia coli*. *Appl. Microbiol. Biotechnol.* 2004, *65*, 538-546.
[42] Jang, H. J., Yoon, S. H., Ryu, H. K., Kim, J. H.*, et al.*, Retinoid production using metabolically engineered *Escherichia coli* with a two-phase culture system. *Microb. Cell. Fact.* 2011, *10*, 10.1186/1475-2859-1110-1159.
[43] Kim, Y. S., Lee, J. H., Kim, N. H., Yeom, S. J.*, et al.*, Increase of lycopene production by supplementing auxiliary carbon sources in metabolically engineered *Escherichia coli*. *Appl. Microbiol. Biotechnol.* 2011, *90*, 489-497.
[44] Gekko, K., Timasheff, S. N., Mechanism of protein stabilization by glycerol: preferential hydration in glycerol-water mixtures. *Biochemistry* 1981, *20*, 4667-4676.
[45] Jarabak, J., Seeds, A. E., Talalay, P., Reversible cold inactivation of a 17*β*-hydroxysteroid dehydrogenase of human placenta: protective effect of glycerol. *Biochemistry* 1966, *5*, 1269-1279.
[46] Durnin, G., Clomburg, J., Yeates, Z., Alvarez, P. J.*, et al.*, Understanding and harnessing the microaerobic metabolism of glycerol in *Escherichia coli*. *Biotechnol. Bioeng.* 2009, *103*, 148-161.
[47] Straathof, A. J., Panke, S., Schmid, A., The production of fine chemicals by biotransformations. *Current Opinion in Biotechnology* 2002, *13*, 548-556.
[48] Hanahan, D., Studies on transformation of *Escherichia coli* with plasmids. *J. Mol. Biol.* 1983, *166*, 557-580.
[49] Studier, F. W., Moffatt, B. A., Use of bacteriophage T7 RNA polymerase to direct selective high-level expression of cloned genes. *J. Mol. Biol.* 1986, *189*, 113-130.
[50] Sambrook, J., Russel, D. W., *Molecular Cloning: A Laboratory Manual*, Cold Spring Harbor Laboratory 2001.
[51] Bachmann, B. J., Derivation and genotypes of some mutant derivatives of *E. coli* K12, in: Umbarger, H. E. (Ed.), *Escherichia coli and Salmonella typhimurium: cellular and molecular biology*, American Society for Microbiology, Washington D. C. 1987, pp. 1191-1219.
[52] Tseng, H. C., Prather, K. L., Controlled biosynthesis of odd-chain fuels and chemicals via engineered modular metabolic pathways. *Proc. Natl. Acad. Sci. USA* 2012, *109*, 17925-17930.
[53] Williams, D. C., McGarvey, D. J., Katahira, E. J., Croteau, R., Truncation of limonene synthase preprotein provides a fully active 'pseudomature' form of this monoterpene cyclase and reveals the function of the amino-terminal arginine pair. *Biochemistry* 1998, *37*, 12213-12220.

Tables

Table 1: List of *E. coli* strains and plasmids used and constructed in this study.

Strain	Relevant characteristics	Reference
E. coli DH5α	F^-, Φ80d*lacZ*ΔM15, Δ(*lacZ*YA-*arg*F)U169, *deoR*, *recA*1, *endA*1, *hsdR*17($r_K^-m_K^+$), *phoA*, *supE*44, λ^-, *thi*-1, *gyr*A96, *relA*1	[48]
E. coli BL21 (DE3)	F^-, *ompT*, $hsdS_B(r_B^-m_B^-)$, *gal* (c1875, *ind*1, *Sam*7, *nin*5, lacUV5-T7 *gene*1), *dcm* (DE3)	[49]
E. coli JM101	*gln*V44, *thi*-1, *supE,* Δ(lac-*proAB*), F'[$lacI^q$ *lacZ*ΔM15 *traD*36 $proAB^+$]	[50]
E. coli MG1655	F^-, λ^-, *ilvG*$^-$, *rfb*-50, *rph*-1	[51]
E. coli MG1655 DE3 (Δ*pta*, Δ*ldh*A, Δ*adh*E)	F^-, λ^-, *ilvG*$^-$, *rfb*-50, *rph*-1,Δ*pta,* Δ*ldhA,* Δ*adhE,* (DE3)	[52]
E. coli SF7N	Δ*ispA*::neo derivative of W3110, Δ(*srl-rec*A) 306::Tn10	[35]
E. coli SF5	Δ(*srl-recA*) 306::Tn10 derivative of W3110	[35]
Plasmids		
pMevT	p15A, Cm^R, P_{lac}, *atoB-erg*13-*tHMGR*1	[16]
pMBIS	pMB1, Tet^R, P_{lac}, *erg*12-*erg*8-*erg*19-*idi*1-*ispA*	[16]
pMVAidi	p15A, Cm^R, P_{lac}, *atoB-erg*13-*tHMGR*1-*erg*12-*erg*8-*erg*19-*idi*1	this study
pMA-T	ColE1, Km^R, holding vector	GeneArt[a]
pMK	ColE1, Km^R, holding vector	GeneArt[a]
pMA-T:KO	ColE1, Km^R, codon-optimized GPPS gene from *Streptomyces* sp. strain KO-3988	this study
pMK:LSAGPPPS2	ColE1, Km^R, truncated and codon-optimized LS gene from *M. spicata* and truncated and codon-optimized GPPS2 gene from *A grandis*	this study
pET24a(+)	ColE1, Km^R, P_{T7}, $lacI^q$	Novagen[c]
pET24:AGPPS2	ColE1, Km^R, P_{T7}, $lacI^q$, truncated and codon-optimized GPPS2 gene from *A. grandis*	this study
pET24:KO	ColE1, Km^R, P_{T7}, $lacI^q$, codon-optimized GPPS gene from *Streptomyces* sp. strain KO-3988	this study
pBAD/Myc-HisA	ColE1, Amp^R, P_{araBAD}, *araC*	Life Technologies[c]

pBAD:LS	ColE1, Amp^R, P_{araBAD}, *araC*, truncated and codon-optimized LS gene from *M. spicata*	this study
pMAL-p5x	pMB1, Amp^R, P_{tac}, $lacI^q$, *malE*	NEB[d]
pTAC:LS	pMB1, Amp^R, P_{tac}, $lacI^q$, truncated and codon-optimized LS gene from *M. spicata*	this study
pTAC:LS:AGPPS2	pMB1, Amp^R, P_{tac}, $lacI^q$, truncated and codon-optimized LS gene from *M. spicata* and truncated and codon-optimized GPPS2 gene from *A. grandis*	this study

[a]GeneArt, (Regensburg, Germany), [b]Novagen, Merck KGaA (Darmstadt, Germany), [c] LifeTechnologies (Darmstadt, Germany), [d] NEB, New England Biolabs (Frankfurt a. M., Germany)
LS: limonene synthase, GPPS: GPP synthase

Table 2: Comparison of limonene production during batch cultivation of different recombinant *E. coli* strains containing the plasmids pMVAidi and pTAC:LS:AGPPS2. The growth rate μ was determined from the initial exponential phase. The theoretical stoichiometric maximum yield with glucose as C source was previously calculated as 0.32 g limonene per g glucose [2].

***E. coli* strain**	**μ/ h^{-1}**	**Limonene/ μmol L_{aq}^{-1}**	**Limonene/ mg L_{aq}^{-1}**	**Spec.yield/ mg g_{cdw}^{-1}**	**$Y_{p/s}$/ mg g^{-1}**	**of max $Y_{p/s}$/ %**
DH5a[a]	0.30	140.2 ± 25.8	19.1 ± 3.5	12.0 ± 2.2	1.9 ± 0.4	0.60
BL21 (DE3)[a]	0.32	111.5 ± 17.7	15.2 ± 2.4	9.5 ± 1.5	1.5 ± 0.2	0.47
JM101[a]	0.34	89.0 ± 2.3	12.2 ± 0.3	7.6 ± 0.2	1.2 ± 0.0	0.38
MG1655 WT[a]	0.32	143.2 ± 5.4	19.5 ± 0.7	12.2 ± 0.5	2.0 ± 0.1	0.61
MG1655 DE3 Δ[a, b]	0.34	81.3 ± 0.0	11.1 ± 0.0	7.0 ± 0.0	1.1 ± 0.0	0.35
SF7N[c]	0.16	139.9 ± 2.8	19.1 ± 0.4	15.1 ± 0.3	1.9 ± 0.0	0.60
SF5[c]	0.16	151.4 ± 5.1	20.6 ± 0.7	17.6 ± 0.6	2.1 ± 0.1	0.64

[a] 50 h, [b] MG1655 DE3 (Δ*pta*, Δ*ldh*A, Δ*adh*E), [c] 72 h

Table 3: K_m values for the respective synthases involved in terpenoid synthesis.

Enzyme	$K_{m(IPP)}$/ µM	$K_{m(DMAPP)}$/ µM	$K_{m(GPP)}$/ µM	Reference
FPP synthase (*E. coli*)	4.0	50	8.7	[33]
GPP synthase 2 (*A. grandis*)	50	90	-	[34]
Limonene synthase (*M. spicata)*	-	-	6.0	[53]

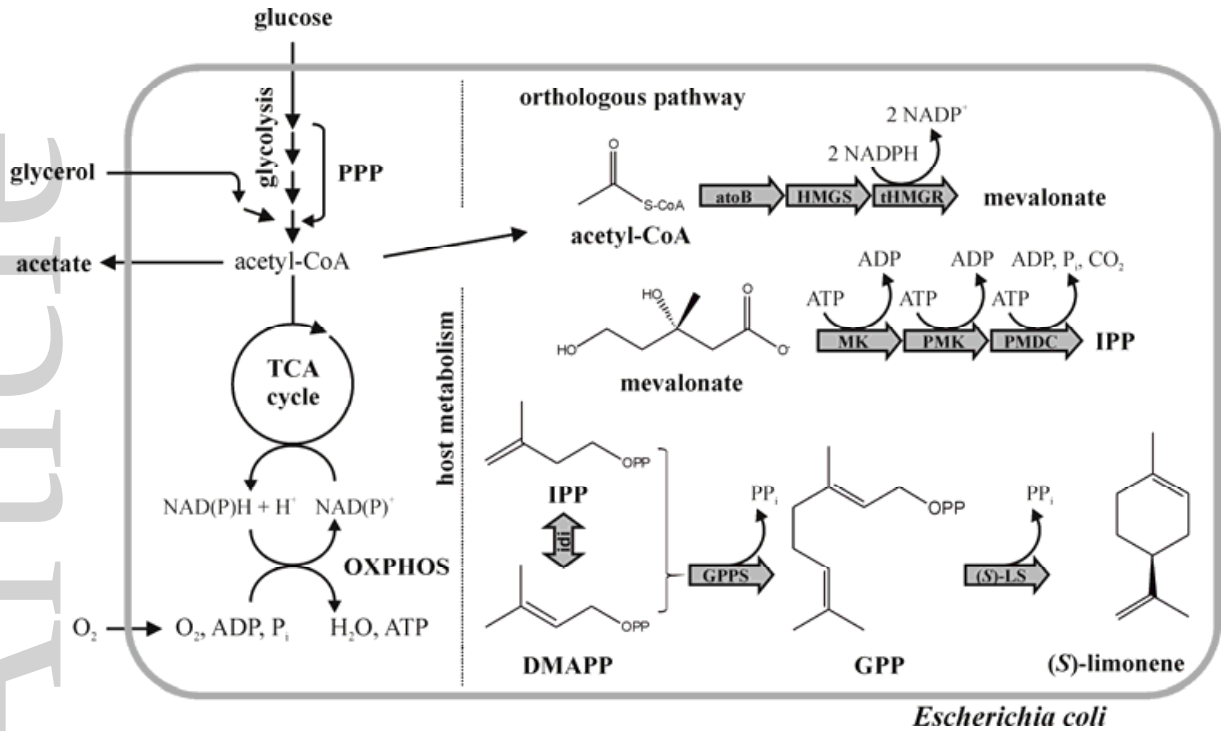

Figure 1: Schematic representation of the primary metabolism and the connection (via acetyl-CoA) to the heterologously integrated pathway for the production of (*S*)-limonene in recombinant *E. coli*. Abbreviations: PPP (pentose phosphate pathway), OXPHOS (oxidative phosphorylation), atoB (acetoacetyl-CoA thiolase), HMGS (3-hydroxy-3-methylglutaryl-CoA synthase), tHMGR (truncated HMG-CoA reductase), MK (mevalonate kinase), PMK (phosphomevalonate kinase), PMDC (diphosphomevalonate decarboxylase), idi (IPP/DMAPP isomerase), IPP (isopentenyl diphosphate), DMAPP (dimethyl allyl diphosphate), GPPS (geranyl diphosphate synthase), GPP (geranyl diphosphate), (*S*)-LS ((*S*)-limonene synthase).

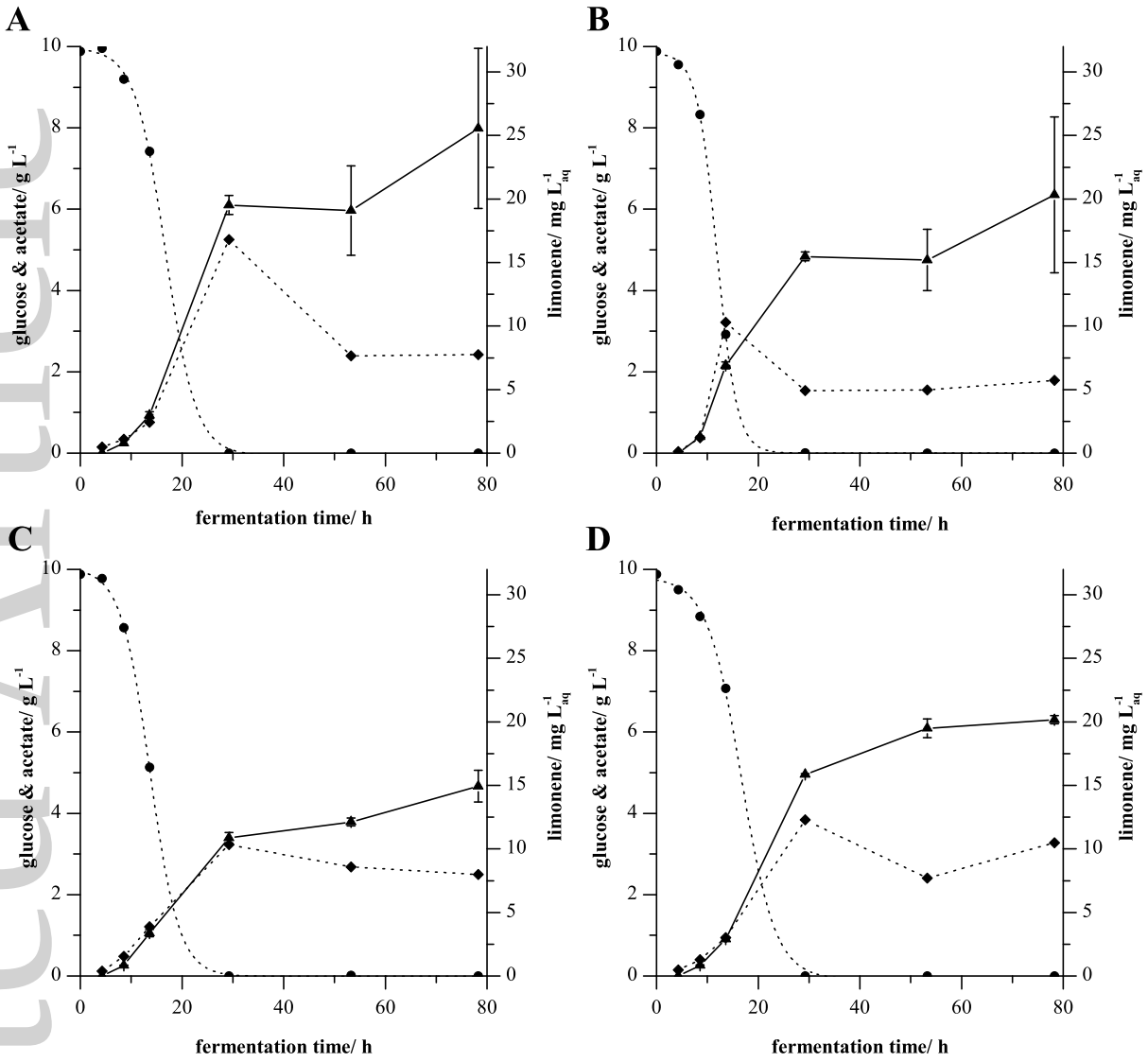

Figure 2: Limonene production in different *E. coli* strains harboring pMVAidi and pTAC:LS:AGPPS2 during two-liquid phase fermentation experiments carried out in a batch culture (M9* medium, 1% (w/v) glucose) with an aqueous:organic phase ratio of 4:1. **A:** *E. coli* DH5α, **B:** *E. coli* BL21 (DE3), **C:** *E. coli* JM101 **D:** *E. coli* MG1655. Glucose (●), acetate (◆) and limonene (▲) concentrations were determined at regular intervals. The glucose data points were subjected to a Boltzmann regression (dotted line). All concentrations relate to the aqueous phase (40 ml). Error bars relate to two independent cultures.

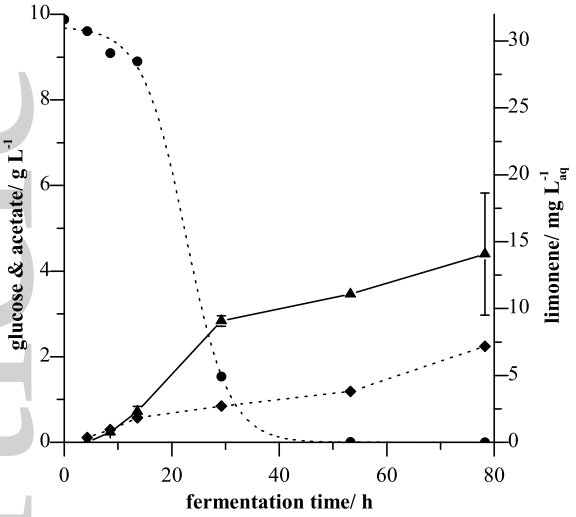

Figure 3: Limonene production in *E. coli* MG1655 DE3 (Δ*pta*, Δ*ldhA*, Δ*adhE*) harboring pMVAidi and pTAC:LS:AGPPS2 during a two-liquid phase fermentation carried out in a batch culture (M9* medium, 1% (w/v) glucose) with an aqueous:organic phase ratio of 4:1. Glucose (●), acetate (◆) and limonene (▲) concentrations were determined at regular intervals. The glucose data points were subjected to a Boltzmann regression (dotted line). All concentrations relate to the aqueous phase (40 ml). Error bars relate to two independent cultures.

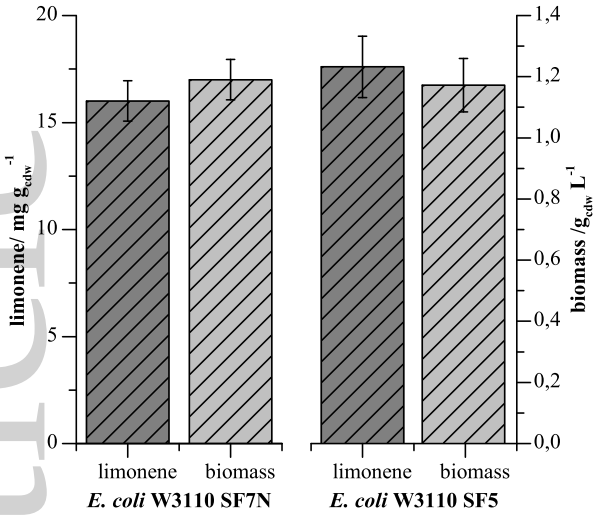

Figure 4: The specific limonene yields (dark grey bars) in *E. coli* SF7N and SF5 harboring pTAC:LS:AGPPS2 and pMVAidi after 72 h with glucose as sole C source. The biomass concentrations (in g_{cdw} L^{-1}) are provided for comparison (light grey bars). Error bars relate to two independent cultures.

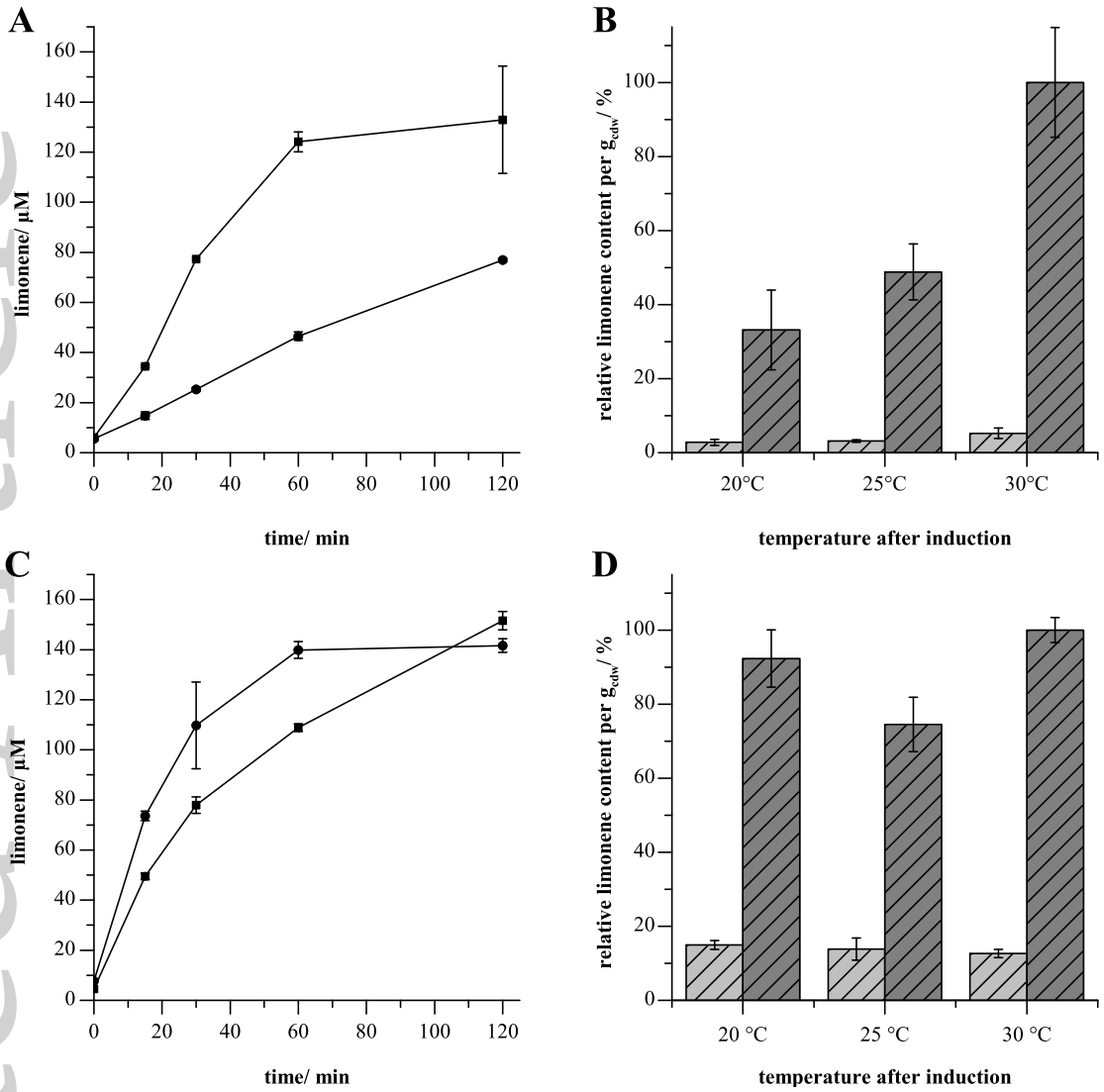

Figure 5: *In vitro* limonene production using cell extracts from *E. coli* BL21 (DE3) (panel **A**) and JM101 (panel **C**) cultures, both harboring pTAC:LS:AGPPS2. The temperature-dependence of *in vivo* limonene production is shown in panel **B** and **D** for strains with pTAC:LS:AGPPS2 (light grey bars), and strains with pTAC:LS:AGPPS2 and pMVAidi (dark grey bars). *In vivo* experiments were run for 48 h after induction in a two-liquid phase system with DINP as inert organic phase (phase ratio 1:4, organic:aqueous volume). Limonene concentrations were normalized to the values obtained at 30°C.

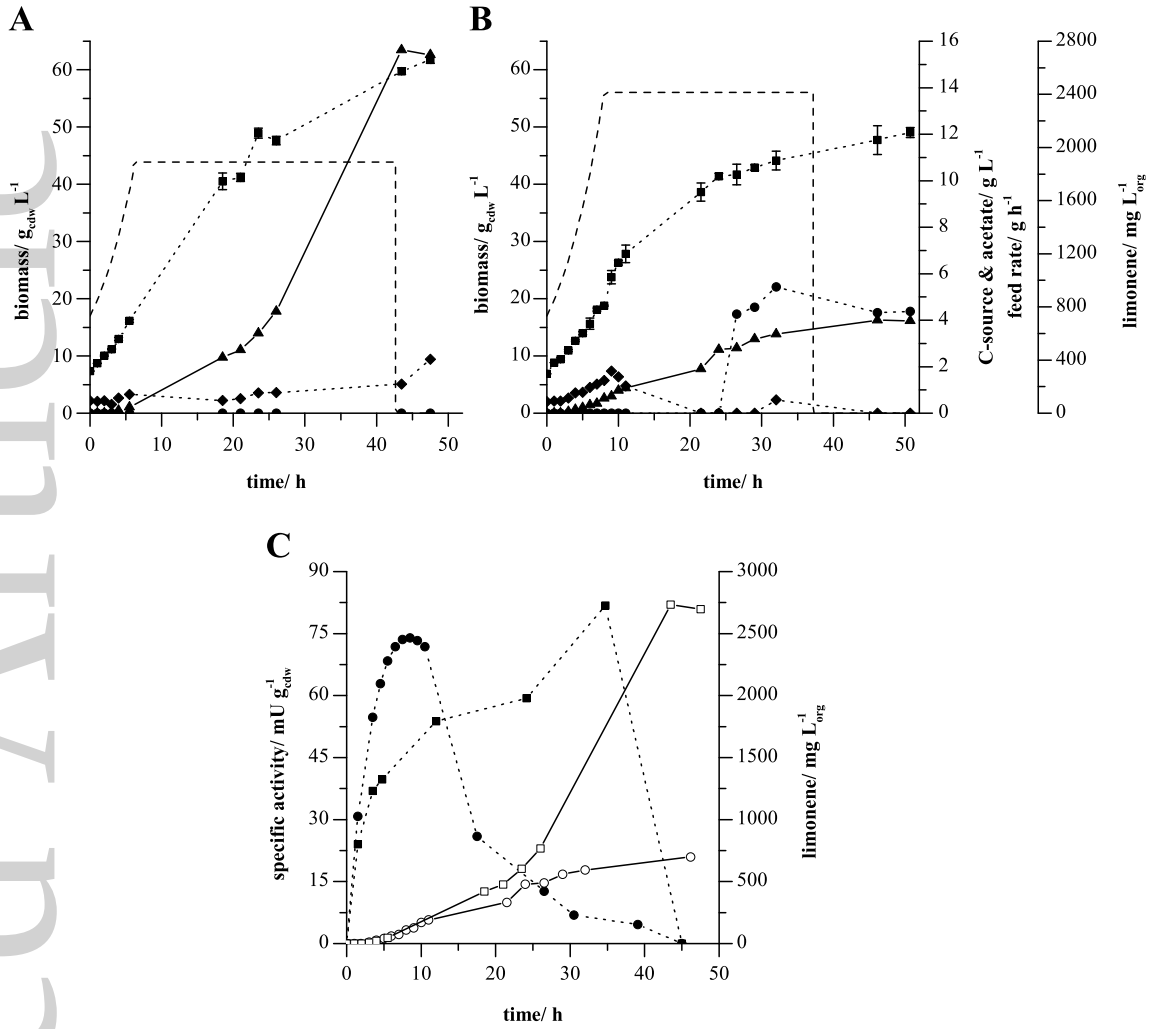

Figure 6: Two-liquid phase fermentation processes with *E. coli* BL21 (DE3) (pMVAidi, pTAC:LS:AGPPS2) cultivated under carbon-limited fed-batch conditions in a 3.1 L reactor (glycerol: panel **A**, glucose: panel **B**). Biomass concentration (■), glycerol or glucose (●) and acetate (◆) concentrations were monitored. The feed rate is given by the dashed line. The limonene concentration (▲) determined by GC relates to the organic phase (0.5 L), because of the changing volume of the aqueous phase during cultivation. The initial phase ratio was set to 1:2 (0.5 L DINP, 1 L M9 medium). The error bars of the biomass concentration are calculated from four measurements. Time point 0 indicates the beginning of fed-batch fermentation. Limonene concentrations of repeated experiments differed by less than ±12%. Panel **C**: Time course of specific activity (closed symbols) and observed limonene concentration (open symbols) during the two-liquid phase fed-batch cultivation of *E. coli* BL21 (DE3) (pMVAidi, pTAC:LS:AGPPS2) under either glycerol- (●, ○) or glucose-limited (■, □) conditions.